PHYSICAL REVIEW D **90,** 014013 (2014)

# Scaling behavior in exclusive meson photoproduction from Jefferson Lab at large momentum transfers

Biplab Dey

*Physik-Institut, Universität Zürich, CH-8057 Zürich, Switzerland*

(Received 27 May 2014; published 9 July 2014)

With the availability of new high-statistics and wide-angle measurements for several exclusive non-$\pi N$ meson photoproduction channels from Jefferson Lab, we examine the fundamental scaling law of 90° scattering in QCD that was originally derived in the high-energy perturbative limit. The data show scaling to be prominently visible even in the medium-energy domain of 2.5 GeV $\lesssim\sqrt{s}\lesssim$ 2.84 GeV, where $\sqrt{s}$ is the center-of-mass energy. While constituent quark exchange suffices for pseudoscalar mesons, additional gluon exchanges from higher Fock states of the hadronic wave functions appear be needed for vector-meson production. The case of the $\phi(1020)$, where two-gluon exchanges are known to dominate, is especially illuminating.

DOI: 10.1103/PhysRevD.90.014013 PACS numbers: 12.38.-t, 12.38.Bx, 13.60.Le

The recent nonperturbative derivation [1] of the power-law behavior of hard scattering amplitudes by Polchinski and Strassler using the AdS/QCD correspondence has opened up new perspectives for nonperturbative QCD. The original derivation of these constituent-counting scaling laws [2,3] was based on the near conformal properties of perturbative QCD (pQCD). The AdS/QCD calculation on the other hand, is an all-orders nonperturbative result. At the few GeV center-of-mass (c.m.) energy regime, the onset of nonperturbative features at lower energies from pQCD at higher energies, often happens within the range of a few hundred MeV in $\sqrt{s}$ (c.m. energy), $\Lambda_{\rm QCD}$ being ≈200 MeV. It is therefore important to investigate the experimental evidence of scaling in the few GeV pQCD to non-pQCD transition energy regime.

Consider the exclusive process $\gamma p\to K^+\Lambda$ as schematically depicted in Fig. 1. This is a useful toy model to study because $|ud\rangle$ is both an isospin and a spin singlet in $\Lambda(|uds\rangle)$ and often behaves as a spectator diquark system. At high $s$, the process is dominated by nonresonant $t$- and $u$-channel processes, where $s=(p_p+p_\gamma)^2$, $t=(p_p-p_\Lambda)^2$, $u=(p_\gamma-p_\Lambda)^2$, and $p_T\sim\sqrt{ut/s}$ is the transverse exchange momentum. The variable $p_T$ sets the time scale $\tau\sim 1/p_T$ for the scattering process. At low $p_T$, there is enough time for the exchanged partons to form bound states (mesons and baryons). In the Regge limit of $t\to 0$ or $u\to 0$, so that $\tau$ is large, these bound states become a tower of states with different angular momenta as given by the corresponding Regge trajectories.

On the other hand, at large $p_T$, the scatterers have very little time and can only exchange partons [4] within themselves. This is the hard scattering limit. It can then be shown [3] from very general pQCD principles that at large $p_T$, for an exclusive process $AB\to CD$ in the limit $s\to\infty$, $t/s$ constant,

$$(d\sigma/dt)_{AB\to CD}\sim s^{-n+2}f(t/s). \tag{1}$$

Here $n=n_A+n_B+n_C+n_D$ is the total number of elementary fields in the initial- and final-state partons. The result derives from the fact that at high $s$ in the limit $|t|\sim|u|\sim s$, there is no other energy scale in the process and each constituent field must scale as $\sqrt{s}$. In the AdS/QCD picture, $n_i$ corresponds to the leading twist dimension $\tau_i$ of the creation operator for the string dual of the $i$th parton.

Since $t=-s(1-\cos\theta_{\rm c.m.})/2$ at large $s$, fixed $t/s$ implies fixed $\cos\theta_{\rm c.m.}$, where $\theta_{\rm c.m.}$ is the meson scattering angle in the c.m. frame. Therefore Eq. (1) can be written as

$$d\sigma/dt\sim s^{-n+2}f(\cos\theta_{\rm c.m.}), \tag{2}$$

and one looks at $\theta=90°$ fixed-angle scattering to extract the scaling power. Assuming only quark exchanges, the above rule predicts $(d\sigma/dt)_{\pi p\to\pi N}\sim s^{-8}$, $(d\sigma/dt)_{pp\to pp}\sim s^{-10}$, and $(d\sigma/dt)_{\gamma p\to\pi N}\sim s^{-7}$. Previous high-energy experiments at SLAC [5], BNL [6] and elsewhere have generally confirmed these predictions. The nonperturbative derivation however implies that as long as there are no $s$-channel resonances present, even at lower energies, hard

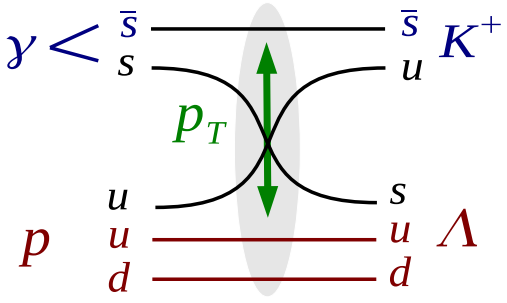


FIG. 1 (color online). The reaction $\gamma p\to K^+\Lambda$ in the parton interchange picture [4]. At high $s$, the transverse momentum $p_T$ sets the time scale for the scattering.

 

scattering amplitudes should still have a simple power-law behavior.

In this article, we probe the "medium-energy" domain of 2.5 GeV $\lesssim\sqrt{s}\lesssim$ 2.84 GeV using six different non-$\pi N$ meson photoproduction channels, viz., $K^+\Sigma^0$, $K^+\Lambda$, $\eta p$, $\eta' p$, $\omega p$ and $\phi p$. Since $\sqrt{s}$ is just above the $s$-channel resonance region, this energy domain is well suited for testing the QCD scaling law in the perturbative-to-nonperturbative transition regime. Our data points comprise recently published high-statistics measurements utilizing the large-angle CLAS spectrometer at Jefferson Lab (JLab) [7–11]. We find that simple scaling behaviors hold for all six channels in this energy region. However, in situations where quark exchanges are suppressed, gluon exchanges occur and higher Fock states with gluonic components could be required. This is true for $\phi$ and $\eta$ which have significant $s\bar{s}$ components and for $\omega$, where Pomeron exchange occurs. The data shows that the extra gluons and Pomerons participating in the scattering process have to be included as additional fields in Eq. (1).

For $K^+\Sigma^0$ photoproduction, earlier SLAC large-angle measurements [5] were only at two energies: $E_\gamma = 4$ and 6 GeV. The new CLAS/JLab results [7] are from production threshold up to $\sqrt{s} = 2.84$ GeV with a wide angular coverage of $-0.95 \le \cos\theta_{\text{c.m.}} \le 0.95$. The CLAS detector acceptance has holes in the extreme forward and backward angles, but is good at most other angles. In particular, the acceptance is very good at mid-angles, which is our current region of interest. The large acceptance of the detector and the high statistics of the data set allowed for fine binning in both energy (10-MeV-wide bins in $\sqrt{s}$) and production angle (0.1 binning in $\cos\theta_{\text{c.m.}}$). Figure 2(a) shows $d\sigma/dt$ plotted vs $s$ and a fit to the function $As^{-C}$. With the $y$ axes set to a logarithmic scale, the power-law behavior is prominent. The exact value of the power $C$ from the fit varies according to where $\sqrt{s}_{\text{min}}$ (the lower energy cutoff) is set for the fit, but it is always found to be around 7, or slightly higher. We can therefore conclude that the $s^{-7}$ prediction from quark counting rules, is followed with reasonable accuracy.

We also examine the $f_{K^+\Sigma^0}(\cos\theta_{\text{c.m.}})$ portion of Eq. (2) by plotting $d\sigma/dt \times s^7$ vs $\cos\theta_{\text{c.m.}}$ in Fig. 2(d). The scaled cross sections appear to line up very well over a wide range of energies. We see a distinct "plateau" at $\theta_{\text{c.m.}} = 90°$ flanked by two "dips" on both sides. The earlier SLAC results [5] reported a similar shape for the $\pi^0 p$ photoproduction channel, whereas, the shape was different for the $\pi^+ n$ case. It can therefore be concluded that the $f(t/s)$ part in Eq. (1) is channel dependent while an $s^{-7}$ scaling seems to be generally applicable here. $f(t/s)$ depends on the form factors of the mesons and baryons [4] and is therefore expected to be channel dependent.

The SLAC paper [5] pointed out that the $K^+\Sigma^0$ and $K^+\Lambda$ cross sections were almost equal at $\theta_{\text{c.m.}} = 90°$. This is also found to be true for the new CLAS results. Above $\sqrt{s} \approx 2.6$ GeV, going from backward to forward $K^+$ production angle, the $\Sigma^0/\Lambda$ cross-section ratio goes from $< 1$ to $> 1$, with $\theta_{\text{c.m.}} = 90°$ being the "cross-over" point where the cross sections are roughly equal. For $K^+\Lambda$, we find the scaling power to be consistent with $C \approx 7$ [Fig. 2(b)], where we caution the reader again that the exact value of $C$ depends on the choice of $\sqrt{s}_{\text{min}}$. The $f_{K^+\Lambda}(\cos\theta_{\text{c.m.}})$ shape [Fig. 2(e)] is found to roughly follow that of $f_{K^+\Sigma^0}(\cos\theta_{\text{c.m.}})$, though the scatter is slightly enhanced in the backward angles.

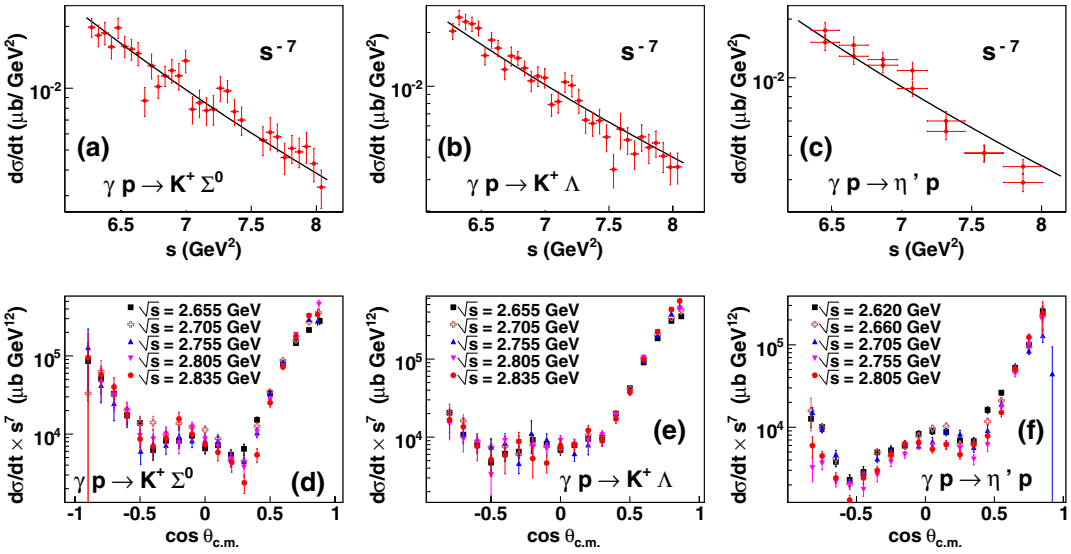


FIG. 2 (color online). The top row shows $d\sigma/dt$ vs $s$ for (a) $K^+\Sigma^0$, (b) $K^+\Lambda$ and (c) $\eta' p$. The black lines show an $As^{-C}$ fit to $d\sigma/dt$ in each individual panel. All three channels demonstrate $\sim s^{-7}$ scaling, as predicted by quark exchange counting rules. The bottom row shows $d\sigma/dt \times s^7$ plotted vs $\cos\theta_{\text{c.m.}}$ over several different $\sqrt{s}$ bins for (d) $K^+\Sigma^0$, (e) $K^+\Lambda$ and (f) $\eta' p$. The collimated set of points reflect the angular dependence $f(\cos\theta_{\text{c.m.}})$ in Eq. (2).

We also note that if the photon dissociates into $s\bar{s}$ in a vector-meson-dominance (VMD)-like picture, then the prediction becomes an $s^{-8}$ scaling.

Previous world data for $\eta' p$ is extremely limited. The JLab results are the first measurements at high $s$ and large $-t$. However, the statistics is limited at higher energies and the $\sqrt{s}$ bins are at least 30 MeV wide. We include data points with $\sqrt{s} \geq 2.5$ GeV and $|\cos\theta_{\mathrm{c.m.}}| \leq 0.05$ here. The scaling fit [Fig. 2(e)] seems to corroborate to a $s^{-7}$ scaling to a fair degree, while the $f_{\eta' p}(\cos\theta_{\mathrm{c.m.}})$ part [Fig. 2(f)] has a strong resemblance with $f_{K^+\Sigma^0}(\cos\theta_{\mathrm{c.m.}})$, and therefore, also with $f_{\pi^0 p}(\cos\theta_{\mathrm{c.m.}})$ from the SLAC results [5].

The $\eta p$ channel is the first instance where we see an appreciable deviation from the predicted $s^{-7}$ scaling from quark counting rules. As for the $\eta' p$, we include all data points with $\sqrt{s} \geq 2.5$ GeV and $|\cos\theta_{\mathrm{c.m.}}| \leq 0.05$. There is appreciable scatter in the data, but a $As^{-C}$ fit suggests the power $C$ to be $\approx$12 or higher. Figure 3(a) shows a particular instance with $C = 12.7$, while $s^{12}d\sigma/dt$ in Fig. 3(d) shows that $f_{\eta p}(\cos\theta_{\mathrm{c.m.}})$ resembles $f_{\eta' p}(\cos\theta_{\mathrm{c.m.}})$ in shape [Fig. 2(f)].

The vector mesons $\omega$ and $\rho$ were studied in earlier JLab analyses. Battaglieri *et al.* reported an $s^{-8}$ scaling for $p\rho$ photoproduction [12] while $s^{-7.2}$ was reported for the $\omega$ [13], though statistics was limited. The SLAC measurements [5] were for combined $(\omega + \rho_0)$ photoproduction, and no scaling power was reported due to extremely poor statistics. The new JLab data has excellent statistics for the $\omega$ channel and points to a $\approx s^{-10}$ ($s^{-9.5}$ is also possible) scaling [Fig. 3(b)]. Qualitatively, $f_{\omega p}(\cos\theta_{\mathrm{c.m.}})$ shows a single tight shape [Fig. 3(e)], reflecting the high precision of the data, but the shape is different from that of $K^+\Sigma^0/\pi^0 p$. There is more or less, a single "dip," similar to the shapes for $\pi^+ n$ and $\pi^-\Delta^{++}$ channels in the SLAC [5] results.

The $\phi p$ channel is of considerable interest in the community because $\phi$ is an almost pure $|s\bar{s}\rangle$ state and thus a potent field to study many novel features. However, the $\phi$ cross section is typically orders of magnitude lower than the $\omega$, for example. Previous world data is thus very sparse and either exists at near-threshold or high-energy forward angles. Since the CLAS detector has the best acceptance in the mid-angles, it was possible to make $\theta = 90°$ measurements keeping a fine enough binning in $\sqrt{s}$.

Figure 3(c) shows the scaling fit for $\phi p$. The data quality is not as precise as the $\omega p$ case due to lower statistics, and $C$ from the fit is at least 12 (or higher). The $s^{12}d\sigma/dt$ plot [Fig. 3(f)] shows a single tight band towards the forward angles. Data in the backward angle is however limited by statistics, though a slight backward-angle rise is visible in $f_{\phi p}(\cos\theta_{\mathrm{c.m.}})$.

Figure 4 shows three ways the reaction $\gamma p \to \phi p$ can proceed at high energies (ignoring the "sea" $s\bar{s}$ content of the proton). At high $s$ and low $-t$, that is, in the diffractive regime, a single soft Pomeron is exchanged [Fig. 4(a)]. In the hard-scattering region, for high $-t$, the mechanism is a two-gluon exchange [Fig. 4(c)] along with a possible "hard" Pomeron exchange [Fig. 4(b)]. For the two-gluon process, the Fock state of the $\phi$ and the incoming photon (in the VMD picture) can each be written as $|s\bar{s}g\rangle$, and that of the protons, as $|uudg\rangle$ ("$g$" signifies a gluon field here). This adds up to a total of $n - 2 = 12$ in Eq. (1), thus

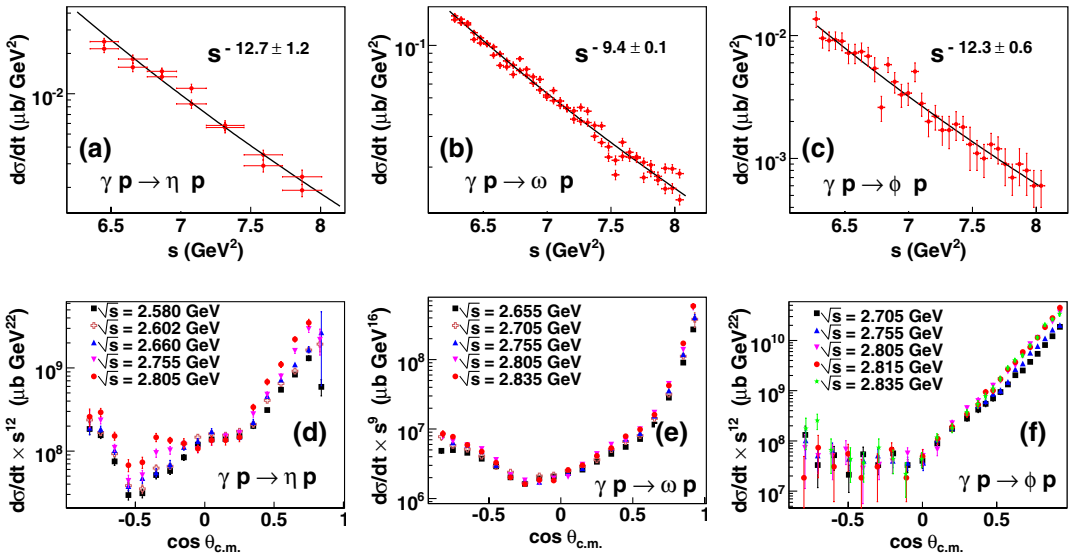


FIG. 3 (color online). Photoproduction channels where $s^{-7}$ scaling, as predicted by quark exchange counting rules, distinctly does not work. The top row shows $d\sigma/dt$ vs $s$ for (a) $\eta p$, (b) $\omega p$ and (c) $\phi p$. The black lines show a $As^{-C}$ fit to $d\sigma/dt$ in each individual panel. The scaling power is different for each meson (see text for explanation). The bottom row shows the scaled cross sections plotted vs $\cos\theta_{\mathrm{c.m.}}$ over several different $\sqrt{s}$ bins for (d) $\eta p$, (e) $\omega p$ and (f) $\phi p$.

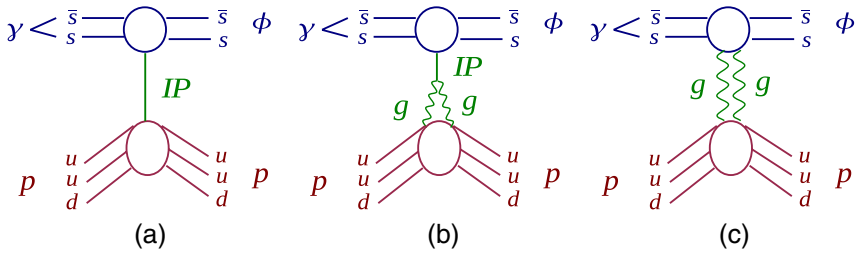


FIG. 4 (color online). The reaction $\gamma p \to p\phi$ at high energies in the VMD model. Panel (a) shows diffractive photoproduction via Pomeron exchange at low $|t|$. Panels (b) and (c) show hard scattering at large $|t|$ where the Pomeron either dissociates into gluonic constituents as in (b) or the direct exchange of two gluons takes place as shown in (c).

explaining the $s^{-12}$-like scaling for the $\phi p$ channel. For the "hard" Pomeron, the same arguments give $s^{-11}$, while for the single Pomeron, a $s^{-10}$ scaling is predicted.

The $\omega p$ channel is known to feature the Pomeron exchange as well (along with $\pi$ and other meson exchanges). From the above argument, it is not surprising therefore, that $\sim s^{-10}$ is seen in this case. Finally, $\eta$, which has more $s\bar{s}$ content than the $\eta'$, will see enhanced gluon exchanges (along with quark interchanges). This explains why (qualitatively, at least) the scaling behavior of $\gamma p \to \eta' p$ is like that of $\gamma p \to \pi N$, while $\gamma p \to \eta p$ "tends towards" the $\gamma p \to \phi p$ behavior.

To summarize, in this paper we have shown that fundamental power-law scaling at 90° scattering is visible in the recent meson photoproduction results from JLab in the 6 GeV energy regime. In the parton interchange model, when additional partons (i.e., other than the constituent quarks) participate in the exchange process, these extra partons can contribute to the dimensional counting as well. This happens when the meson and nucleon have no quarks in common, such as, in $\phi p$ photoproduction, and two-gluon exchanges are required. For the vector mesons $\omega$ and $\rho$, the additional parton can also be a Pomeron. The scaling power laws seen in the JLab data are completely consistent with this physical picture. Furthermore, since $\sqrt{s} < 2.84$ GeV here, which does not quite fall in the "high-energy" domain, the present results also lend experimental credence to the nonperturbative nature of scaling in QCD, as shown by recent calculations using AdS/QCD.

Finally, we note that the present study can be directly extended upon, both in statistical precision and to higher energies with the 12 GeV upgrade program at JLab [14].


[1] J. Polchinski and M. J. Strassler, Phys. Rev. Lett. **88**, 031601 (2002).
[2] V. A. Matveev, R. M. Muradian, and A. N. Tavkhelidze, Lett. Nuovo Cimento **7**, 719 (1973).
[3] S. J. Brodsky and G. L. Farrar, Phys. Rev. Lett. **31**, 1153 (1973); Phys. Rev. D **11**, 1309 (1975).
[4] R. Blankenbecler, S. J. Brodsky, J. F. Gunion, and R. Savit, Phys. Rev. D **8**, 4117 (1973).
[5] R. L. Anderson, D. Gustavson, D. Ritson, G. Weitsch, H. Halpern, R. Prepost, D. Tompkins, and D. Wiser, Phys. Rev. D **14**, 679 (1976).
[6] C. White *et al.*, Phys. Rev. D **49**, 58 (1994).
[7] B. Dey *et al.* (CLAS Collaboration), Phys. Rev. C **82**, 025202 (2010)
[8] M. E. McCracken *et al.* (CLAS Collaboration), Phys. Rev. C **81**, 025201, (2010).
[9] M. Williams *et al.* (CLAS Collaboration), Phys. Rev. C **80**, 045213 (2009).
[10] M. Williams *et al.* (CLAS Collaboration), Phys. Rev. C **80**, 065208 (2009).
[11] B. Dey *et al.* (CLAS Collaboration), Phys. Rev. C **89**, 055208 (2014).
[12] M. Battaglieri *et al.*, Phys. Rev. Lett. **87**, 172002 (2001).
[13] M. Battaglieri *et al.*, Phys. Rev. Lett. **90**, 022002 (2003).
[14] http://www.jlab.org/12GeV/.